



Silk fabric-based wearable thermoelectric generator for energy harvesting from the human body



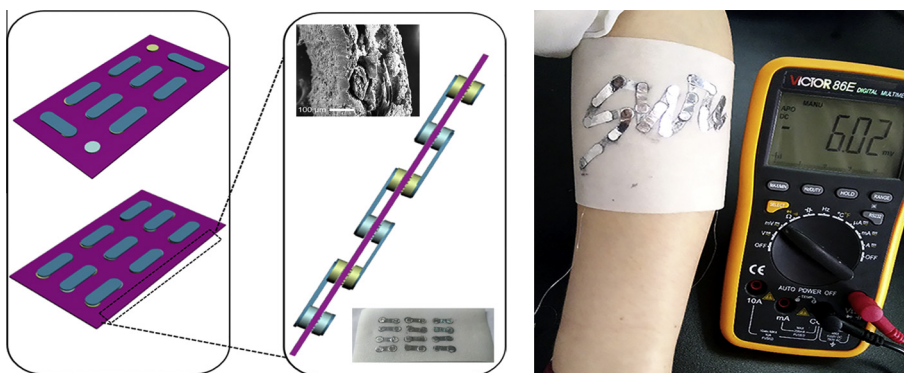
Zhisong Lu^{*}, Huihui Zhang, Cuiping Mao, Chang Ming Li

Chongqing Key Laboratory for Advanced Materials & Technologies of Clean Energies, Southwest University, 1 Tiansheng Road, Chongqing 400715, PR China
Institute for Clean Energy & Advanced Materials, Faculty of Materials & Energy, Southwest University, 1 Tiansheng Road, Chongqing 400715, PR China

HIGHLIGHTS

- A thermoelectric (TE) generator was prepared on commercially available silk fabric.
- The silk fabric-based TE generator could convert thermal energy into electricity.
- Applications of the TE generator for human body heat harvesting were demonstrated.

GRAPHICAL ABSTRACT



ARTICLE INFO

Article history:

Received 4 September 2015
Received in revised form 12 November 2015
Accepted 27 November 2015

Keywords:

Silk
Thermoelectric power generator
Energy harvesting
Wearable electronics
Flexibility

ABSTRACT

The development of flexible thermoelectric (TE) power generators for harvesting energy from the human body has attracted significant interest in recent years. However, thus far, a wearable TE power generator based on commercially available fabrics has not been realized. In this study, nanostructured Bi_2Te_3 and Sb_2Te_3 were synthesized and deposited on both sides of a silk fabric to form TE columns. These TE columns were connected with silver foils to fabricate a prototype integrating an array of 12 thermocouples. The generator could effectively convert thermal energy into electricity in the temperature difference (ΔT) range of 5–35 K. The maximum voltage and power outputs were ~ 10 mV and ~ 15 nW, respectively, with no significant change in both, during 100 cycles of bending and twisting. Different voltage output profiles were collected from an arm-attached generator before and after 30 min of walking, to highlight the immense potential of the silk fabric-based TE generator. This study provides a new approach for developing fabric-based TE power generators for practical applications in wearable electronics.

© 2015 Elsevier Ltd. All rights reserved.

1. Introduction

Rapid advancements in electronics and miniature technology have facilitated the development of multifunctional wearable

devices for real-time health monitoring and fitness tracking in recent years [1–4]. Power-supply systems, which are a critical component, should fulfill the requirements of size, weight, flexibility, and wearability while maintaining their functions [5–7]. Currently, rechargeable lithium-ion (Li-ion) batteries that are compact and lightweight are the most widely utilized energy storage systems for wearable electronics [8–10]. Although they can provide sufficient energy to power the devices, their small size signif-

^{*} Corresponding author at: Institute for Clean Energy & Advanced Materials, Faculty of Materials & Energy, Southwest University, 1 Tiansheng Road, Chongqing 400715, PR China. Tel.: +86 23 68254732; fax: +86 23 68254969.

E-mail address: zslu@swu.edu.cn (Z. Lu).

icantly restricts their capacity and battery life. This has become the main constraint of wearable technology.

Batteries can be combined with wearable generators to harvest energy from the environment or the human body, creating self-chargeable systems for continuous operation of these devices. Thermoelectric (TE) power generators have been developed to harvest energy from waste heat generated by the human body through physical contact with the human skin [11,12]. According to the Seebeck effect, the power output produced by the TE generator is proportional to the thermal gradient between the hot junction that is in contact with the skin and the environment-exposed cold junction [13,14]. Flexible TE power generators containing several pairs of thermocouples have been fabricated on various substrates for heat collection from the human body [15,16]. Polymer films including polyethylene (PE), polydimethylsiloxane (PDMS), polyimide (PI), and Kapton films are the most popular substrates possessing excellent flexibility for use in TE power systems [17–19]. Because both hot and cold junctions can be fabricated only on the same side of the film, the TE generators can be used as skin or cloth-attached devices, and are not directly wearable. Very recently, thermocouples have been deposited on polyester or glass-based fabrics, which have the feasibility to be fabricated in the form of clothing [20]. However, in these studies, specially designed fabric structures with large holes have been utilized to ensure the penetration of TE materials, which cannot be adapted to well-established weaving techniques. Hence, it is highly desirable to develop an approach that could match the existing weaving techniques for the fabrication of wearable fabric-based TE generators. To the best of our knowledge, there are no previous studies on wearable TE power generators based on commercially available fabrics.

Silk from *Bombyx mori* cocoons has been regarded as “the queen of textiles” owing to its softness, high hygroscopicity, and superior skin affinity [21–25]. This fabric has been used to make clothing for thousands of years, and therefore, it is an ideal substrate for the development of wearable TE generators. Bismuth telluride (Bi_2Te_3) and antimony telluride (Sb_2Te_3) are the most widely used TE materials because of their high TE efficiency near room temperature (25 °C) [26,27]. Herein, we present a wearable TE power generator based on commercially available silk fabrics for energy harvesting from waste heat generated by the human body. Nanostructured Bi_2Te_3 and Sb_2Te_3 were synthesized hydrothermally and deposited on both sides of the silk fabric to form TE columns of *n*-type and *p*-type materials. After connecting the columns with silver foils, a prototype, integrating an array of 12 thermocouples was fabricated and evaluated as a wearable TE generator. The effects of repeated bending or twisting on the performance of the generator were examined. The practical applications of silk fabric-based TE generators with designed patterns for the collection of heat energy from the human body are demonstrated in this study.

2. Experimental section

2.1. Chemicals

TeO_2 (metals basis, 99.99%), $\text{Bi}(\text{NO}_3)_3 \cdot 5\text{H}_2\text{O}$ (99.995%), SbCl_3 (AR, 99.98%), polyvinyl pyrrolidone (PVP, MW 58000), $\text{N}_2\text{H}_4 \cdot \text{H}_2\text{O}$ (98%), and ethylene glycol (EG, 99%) were purchased from Aladdin (Shanghai, China). Deionized water (resistance over 18 M Ω cm) was generated by a Millipore Q water purification system.

2.2. Synthesis of nanostructured Bi_2Te_3 and Sb_2Te_3

Nanostructured Bi_2Te_3 and Sb_2Te_3 were synthesized hydrothermally as in previous studies [28–30]. 1.2 g PVP and 6 mmol TeO_2

powder were mixed in 100 mL of EG with vigorous stirring at 200 °C. 0.5 g of NaOH was added to the mixture and stirred for 20 min. Then, 0.6 mL of $\text{N}_2\text{H}_4 \cdot \text{H}_2\text{O}$ was injected into the solution, and the solution was stirred for another 60 min to obtain the Te nanotubes. For the preparation of Bi_2Te_3 , the Bi precursor was reacted with the Te nanotubes for 60 min at 160 °C. The final product was collected by centrifugation at 8500 rpm, and washed several times with water and absolute ethanol. As to the synthesis of Sb_2Te_3 , 0.5 mmol SbCl_3 , 15 mL hydrazine ($\text{N}_2\text{H}_4 \cdot \text{H}_2\text{O}$), and 0.6 mmol Te nanotubes were added to 20 mL deionized water under ultrasonic irradiation at room temperature for 30 min. The mixed solution was heated in a Teflon-lined stainless steel autoclave (50 mL) at 150 °C for 6 h. After cooling to room temperature, the gray-black product was obtained by centrifugation, and it was washed three times using water.

2.3. Characterization of materials

Morphologies of the materials, silk fabrics, and the TE generator devices were imaged using a JSM-6510LV scanning electron microscope (JEOL, Tokyo, Japan) operating at 20 kV. During SEM measurements, EDS (INCA X-Max 250) data were collected to analyze the chemical elements. XRD spectra were examined using a Cu K α -ray with tube conditions at 40 kV and 30 mA ranging from 10° to 80° (XRD-7000, Shimadzu, Japan). Bi_2Te_3 and Sb_2Te_3 pellets with diameters of 10 mm and thicknesses of ~2.5 mm were prepared using spark plasma sintering for measuring the Seebeck coefficient. The voltage across the pellet was measured using a Keithley 2400 multimeter. The Seebeck coefficient was extracted from the slope of the voltage versus temperature difference (ΔT) curves.

2.4. Fabrication of silk-based TE power generator

Fig. 1 shows the fabrication process of a silk-based TE power generator. A 4 cm \times 8 cm silk fabric coated with a layer of polyvinyl alcohol was pricked with a needle to generate holes at the designated locations, to ensure good contact on both the sides of the material. A paste consisting of TE materials (80 mg Bi_2Te_3 or 120 mg Sb_2Te_3), liquid adhesive binder, and deionized water was repeatedly deposited on both the sides of the silk fabric to create TE material columns with a thickness of ~300 μm and a diameter of 4 mm. The as-prepared silk fabrics were vacuum dried at 120 °C for 10 min. Then, conductive silver foils were pasted onto the TE columns with silver paste to connect the *p*-type and *n*-type material columns. A prototype consisting of 12 thermocouples was fabricated for performance measurements.

2.5. Performance evaluation of the silk-based TE power generator

A homemade system consisting of a heating stage and an aluminum-cooling surface was set up for the generation of ΔT , and the characteristic output of the TE generator (Fig. S1 in the Supplementary Information). ΔT from 5 to 35 K was generated using the system. The electrical performance of the TE device was measured using a Victor 86E digital multimeter.

3. Results and discussion

3.1. Characterization of Bi_2Te_3 and Sb_2Te_3 nanomaterials

Because the performance of the TE power generators significantly depends on the TE materials, it is very important to check the quality of the synthesized products. Morphologies of the *p*-type and *n*-type TE nanomaterials were investigated using SEM.

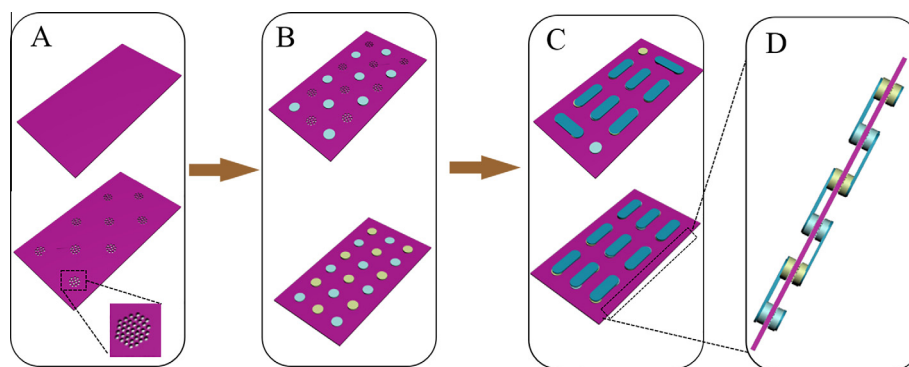


Fig. 1. Schematic illustration of the fabrication process of a silk-based TE power generator. (A) Pretreatment of the silk fabric; (B) deposition of Bi_2Te_3 and Sb_2Te_3 nanomaterials on the silk fabric; (C) connection of *p*-type and *n*-type columns with silver foils; (D) side view of the silk-based TE power generator.

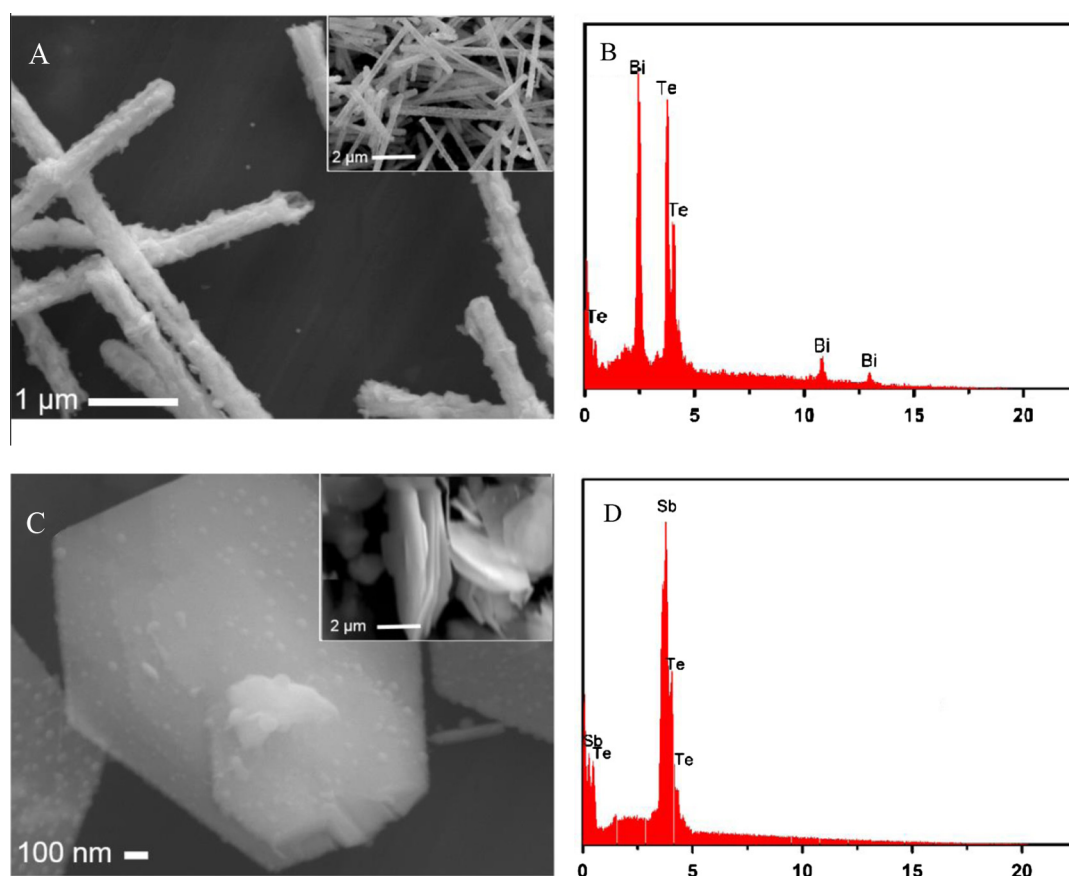


Fig. 2. Morphologies and chemical elements of the as-synthesized Bi_2Te_3 and Sb_2Te_3 nanomaterials. (A) SEM images of Bi_2Te_3 nanotubes; (B) EDX spectrum of Bi_2Te_3 nanotubes; (C) SEM images of Sb_2Te_3 nanoplates; (D) EDX spectrum of Sb_2Te_3 nanoplates. Insets are the corresponding SEM images with lower magnification.

As shown in Fig. 2A, one-dimensional rod-shaped materials $\sim 8 \mu\text{m}$ in length and $\sim 250 \text{ nm}$ in diameter were obtained, and the broken edges exhibit their tubular structures (Fig. S2 in Supplementary Information). The peaks corresponding to Bi and Te elements can be clearly seen in the EDX spectrum (Fig. 2B), which indicates that the as-prepared materials are Bi_2Te_3 nanotubes. The tubular morphology may reduce the lattice thermal conductivity, further enhancing the overall TE properties of Bi_2Te_3 [31]. In Fig. 2C, micrometer-scaled hexagonal nanoplates with a thickness of $\sim 100 \text{ nm}$ are prepared. The EDX spectrum shows that the nanoplates are composed of Sb and Te elements (Fig. 2D), confirming the successful synthesis of *p*-type Sb_2Te_3 nanoplates. The

significantly improved TE properties of the nanoplate-structured Sb_2Te_3 have also been proven in previous literature [32].

Crystal phases of the Bi_2Te_3 nanotubes and Sb_2Te_3 nanoplates were further characterized with XRD. Fig. 3A and B exhibit the typical XRD patterns of the Bi_2Te_3 nanotubes and Sb_2Te_3 nanoplates, respectively, which can be readily indexed to phases of pure Bi_2Te_3 (JCPDS No. 15-863) and pure Sb_2Te_3 (JCPDS No. 15-0874). The desired nanoscale morphologies and the excellent crystalline structures may guarantee the TE properties of both *p*-type Sb_2Te_3 and *n*-type Bi_2Te_3 . TE material pellets with a diameter of 10 mm and a thickness of $\sim 2.5 \text{ mm}$ were prepared under a pressure of 40 MPa for the measurement of the Seebeck coefficient. Seebeck

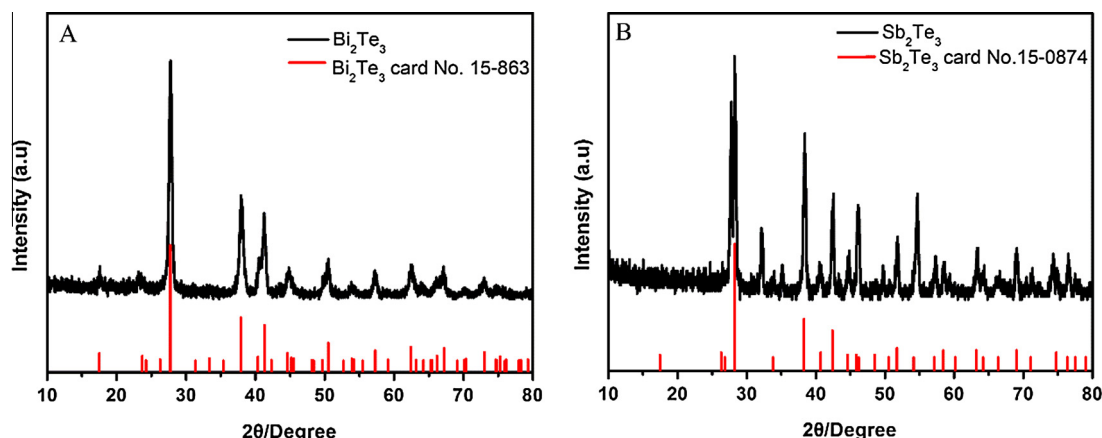


Fig. 3. XRD patterns of the (A) Bi_2Te_3 nanotubes and (B) Bi_2Te_3 nanoplates.

coefficients of *n*-type Bi_2Te_3 and *p*-type Sb_2Te_3 are -0.0368 and 0.1108 mV K^{-1} , respectively (Table 1).

3.2. Characterization of the silk fabric-based TE power generator

A silk fabric-based TE power generator was fabricated step-by-step as shown in Fig. 4. Twelve thermocouples are connected with silver foils to produce the final device. The deposition of TE nanomaterials is the most critical procedure during the fabrication process. To ensure the efficient deposition and the effective contact of the TE nanomaterials on both sides of the silk fabric, morphologies of Bi_2Te_3 nanotubes and Sb_2Te_3 nanoplates on silk fabric are investigated with SEM. Several silk fibers, $\sim 5 \mu\text{m}$ in size, are twisted together to make yarns that are tightly interlocked with each other to form a silk fabric (Fig. 5A). After the deposition of TE nanomaterials, dense films can be observed at the designated places (Fig. 5B and D). SEM images with high magnification show that the films are composed of Bi_2Te_3 nanotubes and Sb_2Te_3 nanoplates, respectively (Fig. 5C and E). The cross-sectional view shows that the thickness of the film is $\sim 50 \mu\text{m}$. The TE nanomaterials deposited on both sides are interconnected through the pores to form a TE material column $\sim 300 \mu\text{m}$ thick (Fig. 5F). In comparison to the millimeter-sized holes on the polyester fabric in the reported study [33], the silk fabric can provide sufficient supports for the attachment of TE materials. Dense packing and contact of the TE nanomaterials on both sides are very important for the fabrication of the silk-based TE power generator without the use of external supports.

3.3. Performance of silk fabric-based TE power generators

Fig. 6A displays the setup of the homemade system for the generation of temperature difference. One side of a silk fabric-based TE generator is in close contact with the heating stage and the other with the aluminum cooling pad for the measurement of voltage and power output. The open-circuit voltage gradually increases from ~ 5 to $\sim 10 \text{ mV}$ as ΔT increases from 5 to 35 K. There is a linear relationship between the voltage and the temperature difference (Fig. 6B). The power output of the device also demonstrates a sim-

ilar trend. The power output linearly rises from ~ 4 to $\sim 15 \text{ nW}$ with the increase in the ΔT (Fig. 6B). It should be noted that the voltage output might decrease when the generator is connected to a load in practical applications (Fig. S3 in Supporting Information). The results verify that the silk fabric-based TE power generator could effectively work to convert thermal energy into electricity in the ΔT range of 5–35 K. At normal physiological conditions, human body temperature is stable at around 37°C . The normal temperature of a habitable environment may vary from 5 to 40°C . Thus, the ΔT range of the power generator should be less than 35 K. Based on Fig. 6B, it can be calculated that the Seebeck coefficient of the device is $\sim 0.16 \text{ mV/K}$, which is significantly lower than the sum of the parameter from 12 Sb_2Te_3 – Bi_2Te_3 thermocouples. The existence of a liquid adhesive binder and low-density values of the pellets formed by the deposition method may cause considerable losses in the Seebeck coefficient.

Because the silk fabric-based TE power generator is designed as a potential power supply system for wearable devices, bending and twisting are unavoidable in its practical applications. Thus, the effects of bending and twisting on the performance of the generator were investigated in this study at $\Delta T = 20 \text{ K}$. It was found that both the voltage and the resistance of the device were stable during 100 cycles of bending (Fig. 7A). Similar to the findings of the bending test, there was no significant change in the voltage during 100 cycles of twisting. However, the resistance slightly increases after 20 twisting cycles, and then, it remains unchanged during the next 80 cycles of twisting (Fig. 7B). The increase in the resistance of the device is less than 10% after 100 cycles of twisting, which is still acceptable for practical usage. The contact resistance created by the silver paste is approximately 50Ω , which is much lower than the device resistance. Thus, the use of silver paste may not significantly affect the final performance of the generator. During device fabrication, *p*-type and *n*-type materials were deposited on both sides of the silk fabric. The contact resistance between the two sides of the TE material may greatly limit the power output of the devices.

3.4. Energy harvesting from the human body

An increase in body temperature usually occurs after exercise, which may lead to a high ΔT across the TE generator. Therefore, the voltage outputs of an arm-attached generator were monitored before and after 30 min of walking ($\sim 4 \text{ km/h}$ for 30 min) (Fig. 8A). A significant increase in the voltage output was observed when the device was attached to the arm. Five to 35 s after the device was attached, the voltage continuously decreased and finally stabilized. The temperature equilibrium across the cold and hot junctions of

Table 1
Seebeck coefficients of the thermoelectric materials (at $T = 310 \text{ K}$).

Thermoelectric materials	Seebeck coefficient (mV K^{-1})
Bi_2Te_3 (<i>n</i> -type)	-0.0368
Sb_2Te_3 (<i>p</i> -type)	0.1108

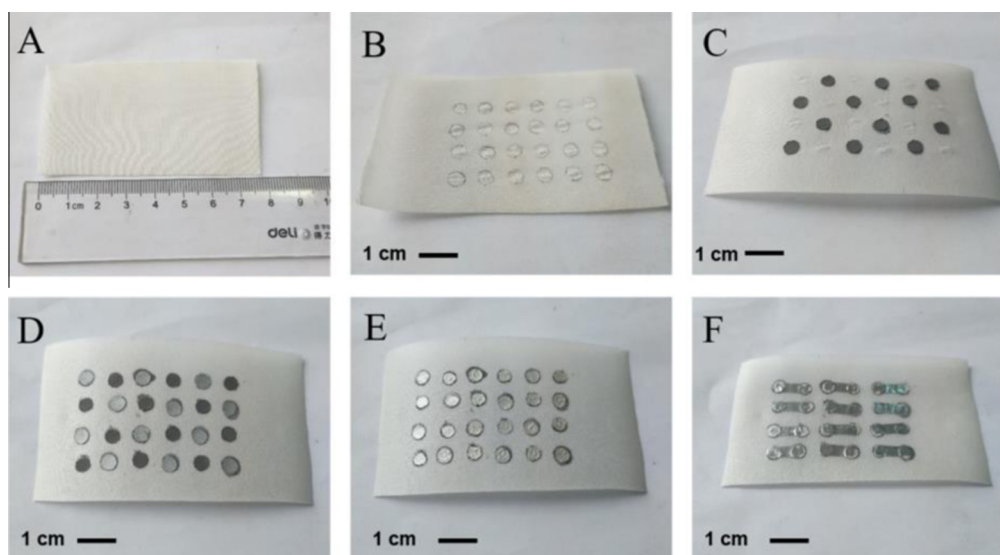


Fig. 4. From a silk fabric to a silk fabric-based TE power generator. (A) A 4 cm × 8 cm silk fabric; (B) the silk fabric after pricking holes at the designated places and after deposition of (C) Bi_2Te_3 nanotubes; and (D) Sb_2Te_3 nanoplates at the places with holes; (E) coating silver paste on the TE material columns; (F) connection of the TE material columns with silver foils.

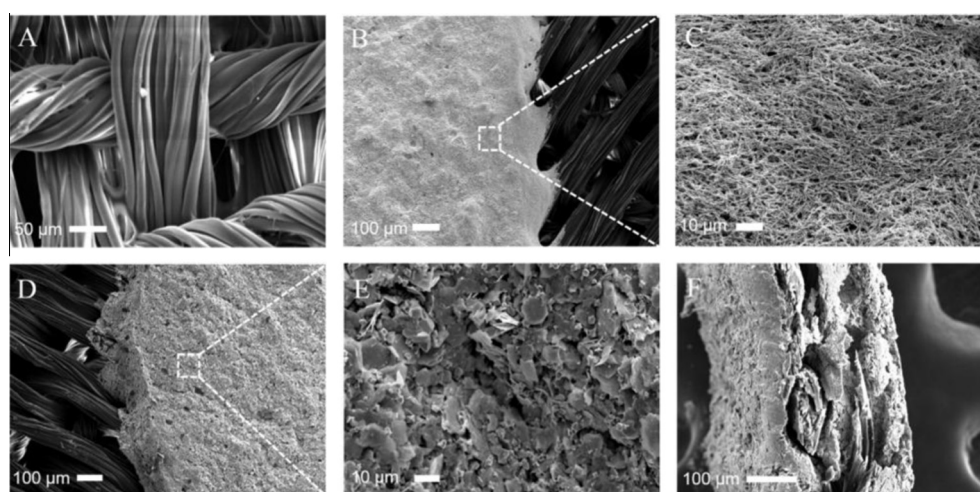


Fig. 5. SEM images of (A) pristine silk fabric; silk fabric with surface-deposited Bi_2Te_3 nanotubes at (B) low; and (C) high magnifications; silk fabric with surface-deposited Sb_2Te_3 nanoplates at (D) low; and (E) high magnifications; as well as (F) the cross-sectional view of a TE nanomaterial column.

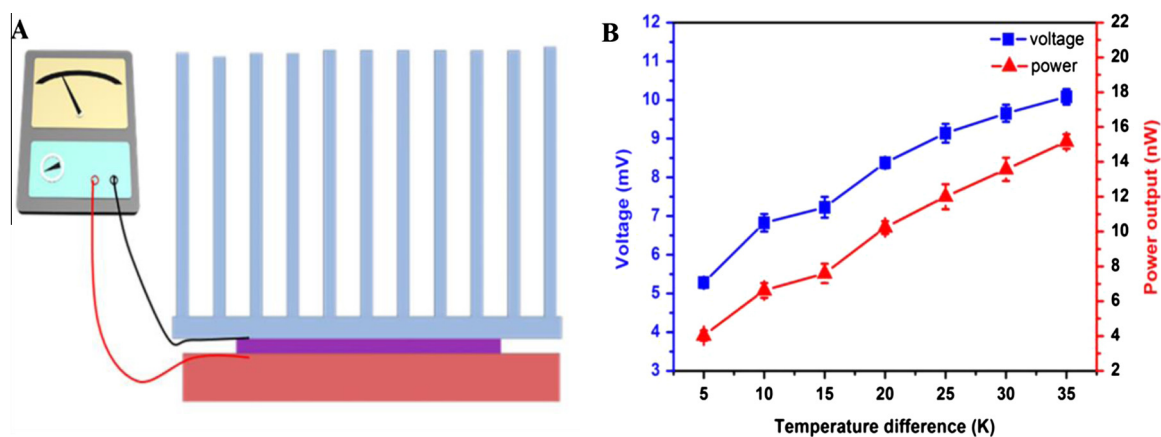


Fig. 6. (A) Schematic diagram of the homemade measurement system; (B) output characteristics of a silk fabric-based TE power generator.

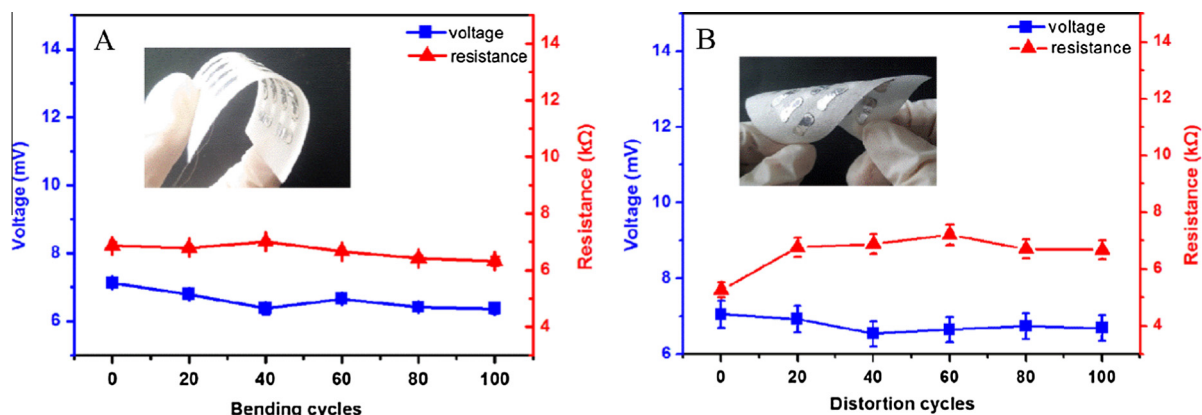


Fig. 7. Effects of bending (A) and twisting (B) on the internal resistance and voltage output of the silk-based TE power generator at $\Delta T = 20$ K; insets show the bending and twisting of a real device, respectively.

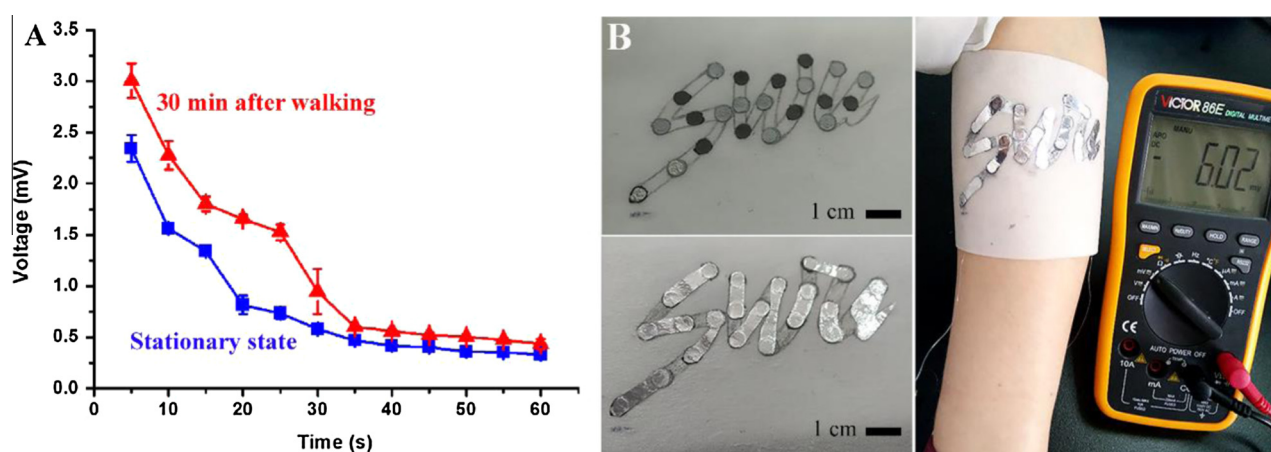


Fig. 8. (A) Voltage outputs of a silk-based TE power generator attached on the human body before (blue line) and after 30 min of walking (red line) at 20°C ; (B) a specially designed silk-based TE generator and its voltage output when attached to the arm at 20°C . (For interpretation of the references to colour in this figure legend, the reader is referred to the web version of this article.)

the power generator may cause voltage reduction. Initially, the body temperature is significantly higher than that of the environment, generating a large voltage output. However, as the heat is gradually transferred from the skin to the environment-exposed side, ΔT becomes small, resulting in the decrease of the voltage. Once temperature equilibrium is reached, the voltage output becomes constant. Interestingly, after exercise, the voltage output is obviously higher than that from a stationary wearer during a time interval of 5–30 s. The results indicate that the device could effectively harvest waste heat from the human body. Moreover, a mobile wearer could provide more heat energy to the TE generator for conversion. The TE power generator could be combined with conventional printing technology to make designed patterns on clothes. As shown in Fig. 8B, an 11-thermocouple based TE power generator was fabricated on a silk fabric to produce the three letters “swu”, which is the abbreviation of Southwest University. When the TE module is attached to the arm, it can generate a voltage output of 6.02 mV.

4. Conclusions

In this study, a wearable TE power generator based on commercially available silk fabrics was developed for harvesting energy from the waste heat generated from the human body. Bi_2Te_3 (*n*-type) nanotubes and Sb_2Te_3 (*p*-type) nanoplates were

hydrothermally synthesized and deposited at designated places on a silk fabric to form TE material columns. To ensure the efficient contact of TE materials on both sides, a number of pores were pricked at the designated places. After connecting the columns with silver foils, a TE generator consisting of 12 thermocouples was fabricated. The dense packing and close contact of the TE nanomaterials on both sides contribute to the tight adherence of the TE columns on the silk fabric. The silk fabric-based TE power generator could effectively convert thermal energy into electricity in the ΔT range of 5–35 K. The maximum voltage and power outputs are ~ 10 mV and ~ 15 nW, respectively. The performance of the device does not change significantly during 100 cycles of bending and twisting. It is demonstrated that a mobile wearer can provide more heat energy to the TE generator for conversion and the TE power generator could be combined with conventional printing technology to make designed patterns on clothes. This study provides a new approach to developing fabric-based TE power generators, which could be combined with rechargeable batteries to create self-chargeable systems for continuous operation of wearable devices in practical applications.

Acknowledgements

This work is financially supported by National Natural Science Foundation of China (Nos. 21205097 and 31200700), Chongqing

Key Laboratory for Advanced Materials and Technologies of Clean Energies under cstc2011pt-sy90001 and Fundamental Research Funds for the Central Universities under XDK2015B016. Z.S. Lu would like to thank the supports by the Specialized Research Fund for the Doctoral Program of Higher Education (RFDP) (Grant No. 20130182120025) and Young Core Teacher Program of the Municipal Higher Educational Institution of Chongqing.

Appendix. A. supplementary material

Supplementary data associated with this article can be found, in the online version, at <http://dx.doi.org/10.1016/j.apenergy.2015.11.038>.

References

- [1] Son D, Lee J, Qiao S, et al. Multifunctional wearable devices for diagnosis and therapy of movement disorders. *Nat Nanotechnol* 2014;9(5):397–404.
- [2] Yao S, Zhu Y. Wearable multifunctional sensors using printed stretchable conductors made of silver nanowires. *Nanoscale* 2014;6(4):2345–52.
- [3] Pang C, Lee C, Suh KY. Recent advances in flexible sensors for wearable and implantable devices. *J Appl Polym Sci* 2013;130(3):1429–41.
- [4] Aboutalebi SH, Jalili R, Esrafilzadeh D, et al. High-performance multifunctional graphene yarns: toward wearable all-carbon energy storage textiles. *ACS Nano* 2014;8(3):2456–66.
- [5] Zhou C, Tu C, Tian J, et al. A low power miniaturized monitoring system of six human physiological parameters based on wearable body sensor network. *Sensor Rev* 2015;35(2):210–8.
- [6] Kim BJ, Kim DH, Lee YY, et al. Highly efficient and bending durable perovskite solar cells: toward a wearable power source. *Energy Environ Sci* 2015;8(3):916–21.
- [7] Drysdale B, Wu J, Jenkins N. Flexible demand in the GB domestic electricity sector in 2030. *Appl Energy* 2015;139:281–90.
- [8] Li N, Chen Z, Ren W, et al. Flexible graphene-based lithium ion batteries with ultrafast charge and discharge rates. *P Natl Acad Sci* 2012;109(43):17360–5.
- [9] Kim SW, Seo DH, Ma X, et al. Electrode materials for rechargeable sodium-ion batteries: potential alternatives to current lithium-ion batteries. *Adv Energy Mater* 2012;2(7):710–21.
- [10] Hu L, La Mantia F, Wu H, et al. Lithium-ion textile batteries with large areal mass loading. *Adv Energy Mater* 2011;1(6):1012–7.
- [11] Madan D, Wang Z, Wright PK, et al. Printed flexible thermoelectric generators for use on low levels of waste heat. *Appl Energy* 2015;156:587–92.
- [12] He W, Zhang G, Zhang X, et al. Recent development and application of thermoelectric generator and cooler. *Appl Energy* 2015;143:1–25.
- [13] Xiao J, Yang T, Li P, et al. Thermal design and management for performance optimization of solar thermoelectric generator. *Appl Energy* 2012;93:33–8.
- [14] Montecucco A, Siviter J, Knox AR. Constant heat characterisation and geometrical optimisation of thermoelectric generators. *Appl Energy* 2015;149:248–58.
- [15] Kim MY, Oh TS. Thermoelectric power generation characteristics of a thin-film device consisting of electrodeposited n-Bi₂Te₃ and p-Sb₂Te₃ thin-film legs. *J Electron Mater* 2013;42(9):2752–7.
- [16] Date A, Date A, Dixon C, et al. Progress of thermoelectric power generation systems: prospect for small to medium scale power generation. *Renew Sust Energy Rev* 2014;33:371–81.
- [17] Francioso L, De Pascali C, Bartali R, et al. PDMS/Kapton interface plasma treatment effects on the polymeric package for a wearable thermoelectric generator. *ACS Appl Mater Int* 2013;5(14):6586–90.
- [18] We JH, Kim SJ, Cho BJ. Hybrid composite of screen-printed inorganic thermoelectric film and organic conducting polymer for flexible thermoelectric power generator. *Energy* 2014;73:506–12.
- [19] Suemori K, Hoshino S, Kamata T. Flexible and lightweight thermoelectric generators composed of carbon nanotube–polystyrene composites printed on film substrate. *Appl Phys Lett* 2013;103(15):153902.
- [20] Kim SJ, We JH, Cho BJ. A wearable thermoelectric generator fabricated on a glass fabric. *Energy Environ Sci* 2014;7(6):1959–65.
- [21] Kalia S, Thakur K, Celli A, et al. Surface modification of plant fibers using environment friendly methods for their application in polymer composites, textile industry and antimicrobial activities: a review. *J Environ Chem Eng* 2013;1(3):97–112.
- [22] Lu Z, Meng M, Jiang Y, et al. UV-assisted in situ synthesis of silver nanoparticles on silk fibers for antibacterial applications. *Colloid Surf A* 2014;447:1–7.
- [23] Lu Z, Mao C, Meng M, et al. Fabrication of CeO₂ nanoparticle-modified silk for UV protection and antibacterial applications. *J Colloid Interface Sci* 2014;435:8–14.
- [24] Lu Z, Xiao J, Wang Y, et al. In situ synthesis of silver nanoparticles uniformly distributed on polydopamine-coated silk fibers for antibacterial application. *J Colloid Interface Sci* 2015;452:8–14.
- [25] Lu Z, Mao C, Zhang H. Highly conductive graphene-coated silk fabricated via a repeated coating-reduction approach. *J Mater Chem C* 2015;3(17):4265–8.
- [26] Kim MY, Oh TS. Preparation and characterization of Bi₂Te₃/Sb₂Te₃ thermoelectric thin-film devices for power generation. *J Electron Mater* 2014;43(6):1933–9.
- [27] Huang B, Lawrence C, Gross A, et al. Low-temperature characterization and micropatterning of coevaporated Bi₂Te₃ and Sb₂Te₃ films. *J Appl Phys* 2008;104(11):113710–1.
- [28] Zhang G, Kirk B, Jauregui LA, et al. Rational synthesis of ultrathin n-type Bi₂Te₃ nanowires with enhanced thermoelectric properties. *Nano Letters* 2011;12(1):56–60.
- [29] Srivastava P, Singh K. Low temperature synthesized thermoelectric Sb₂Te₃ irregular nanoflakes. *Mater Lett* 2012;75:42–4.
- [30] Yang JS, Zuo PF, Zhang SY, et al. Sb₂Te₃ nanoplates: preparation, reaction mechanism and electrochemical property. *J Alloy Comp* 2013;565:73–8.
- [31] Li Z, Zheng S, Huang T, et al. Rational design, high-yield synthesis, and low thermal conductivity of Te/Bi₂Te₃ core/shell heterostructure nanotube composites. *J Alloy Comp* 2014;617:247–52.
- [32] Schulz S, Heimann S, Friedrich J, et al. Synthesis of hexagonal Sb₂Te₃ nanoplates by thermal decomposition of the single-source precursor (Et₂Sb) ₂Te. *Chem Mater* 2012;24(11):2228–34.
- [33] Kim MK, Kim MS, Lee S, et al. Wearable thermoelectric generator for harvesting human body heat energy. *Smart Mater Struct* 2014;23(10):105002.